

# Analysis of the *Pseudomonas aeruginosa* Regulon Controlled by the Sensor Kinase KinB and Sigma Factor RpoN

F. Heath Damron,<sup>a,c,d</sup> Joshua P. Owings,<sup>d</sup> Yuta Okkotsu,<sup>e</sup> John J. Varga,<sup>d</sup> Jill R. Schurr,<sup>f</sup> Joanna B. Goldberg,<sup>d</sup> Michael J. Schurr,<sup>e</sup> and Hongwei D. Yu<sup>a,b,c</sup>

Departments of Biochemistry and Microbiology<sup>a</sup> and Pediatrics,<sup>b</sup> Joan C. Edwards School of Medicine, Marshall University, Huntington, West Virginia, USA; Progenesis Technologies, LLC, Huntington, West Virginia, USA<sup>c</sup>; Department of Microbiology, Immunology, and Cancer Biology, University of Virginia, Charlottesville, Virginia, USA<sup>d</sup>; Department of Microbiology, School of Medicine, University of Colorado, Aurora, Colorado, USA<sup>e</sup>; and Affymetrix, Inc., Santa Clara, California, USA<sup>f</sup>

**Alginate overproduction by *Pseudomonas aeruginosa*, also known as mucoidy, is associated with chronic endobronchial infections in cystic fibrosis. Alginate biosynthesis is initiated by the extracytoplasmic function sigma factor ( $\sigma^{22}$ ; AlgU/AlgT). In the wild-type (wt) nonmucoid strains, such as PAO1, AlgU is sequestered to the cytoplasmic membrane by the anti-sigma factor MucA that inhibits alginate production. One mechanism underlying the conversion to mucoidy is mutation of *mucA*. However, the mucoid conversion can occur in wt *mucA* strains via the degradation of MucA by activated intramembrane proteases AlgW and/or MucP. Previously, we reported that the deletion of the sensor kinase KinB in PAO1 induces an AlgW-dependent proteolysis of MucA, resulting in alginate overproduction. This type of mucoid induction requires the alternate sigma factor RpoN ( $\sigma^{54}$ ). To determine the RpoN-dependent KinB regulon, microarray and proteomic analyses were performed on a mucoid *kinB* mutant and an isogenic nonmucoid *kinB rpoN* double mutant. In the *kinB* mutant of PAO1, RpoN controlled the expression of approximately 20% of the genome. In addition to alginate biosynthetic and regulatory genes, KinB and RpoN also control a large number of genes including those involved in carbohydrate metabolism, quorum sensing, iron regulation, rhamnolipid production, and motility. In an acute pneumonia murine infection model, BALB/c mice exhibited increased survival when challenged with the *kinB* mutant relative to survival with PAO1 challenge. Together, these data strongly suggest that KinB regulates virulence factors important for the development of acute pneumonia and conversion to mucoidy.**

The genetic disease cystic fibrosis (CF) manifests in multiple systems of the body; the most life-threatening complication is the predisposition to bacterial respiratory infections (25). In decades past, *Staphylococcus aureus* and *Haemophilus influenzae* were recognized as the dominant pathogens that infected the CF patient airway. Antibiotic therapies have decreased the incidence of these pathogens. However, infection of the CF patient's airway with the Gram-negative opportunistic pathogen *Pseudomonas aeruginosa* remains of great concern. Once *P. aeruginosa* colonizes the lung, it multiplies to high cell densities and forms biofilms, where neither the host immune response nor antibiotic therapies are effective in complete eradication of the organism.

*P. aeruginosa* has numerous genes and phenotypes that contribute to the persistence in the CF lung. The phenotype known as mucoidy is caused by the overproduction of the exopolysaccharide alginate. Typically, nonmucoid environmental strains initially colonize the lungs of CF patients. However, isolation of stable mucoid strains from sputum samples signals the onset of chronic infection of the CF lung (25). One of the master regulators of alginate production is the sigma factor  $\sigma^{22}$  also known as AlgU (AlgT). AlgU activates alginate overproduction by regulating the expression of transcription factors (2, 16, 23) leading to transcriptional activation of the *algD* biosynthetic operon (17, 26, 36). The genes controlled by AlgU and their role in the alginate machinery have been extensively reviewed elsewhere (46). MucA is an anti-sigma factor and the primary negative regulator of alginate overproduction. MucA directly sequesters AlgU to the inner membrane (48). Constitutively mucoid CF isolates typically harbor mutations in *mucA* (36), but mutations in the other negative regulators of AlgU, *mucB* and *mucD*, have been identified in mucoid CF isolates (8). If the *mucA* gene is wild type (wt), MucA must be

proteolytically degraded to activate AlgU (45). MucA can be degraded by proteases AlgW and MucP, which are the homologues of *Escherichia coli* DegS and RseP (45). AlgW protease can be activated by accumulation of envelope proteins (45). Once an envelope protein binds to and activates AlgW, cleavage of MucA occurs at several specific residues in the periplasmic C terminus of MucA (6). After AlgW cleavage of MucA, it is hypothesized that MucP will then further digest MucA (45), which could activate AlgU. An exception has been observed where it appears that MucP can cleave MucA independent of AlgW (13). MucB and MucD also participate in modulating AlgU activity through regulated proteolytic degradation of MucA. MucB (24, 36) protects the C terminus of MucA from proteolytic degradation (6), and MucD is a chaperone protease (58, 63) that regulates protein quality in the periplasm, which may indirectly control MucA degradation (13).

The mucoid phenotype can also be regulated via environmental sensing. Environmental nonmucoid strains have the capacity to become mucoid regardless of *mucA* mutation (10). One method used by bacteria to sense the environment is through two-component regulatory systems which are comprised of a cytoplasmic membrane-bound histidine kinase, a sensor, and a response regulator, usually a transcription factor. Phosphorylation and de-

Received 31 August 2011 Accepted 23 December 2011

Published ahead of print 30 December 2011

Address correspondence to Hongwei D. Yu, yuh@marshall.edu.

Supplemental material for this article may be found at <http://jb.asm.org/>.

Copyright © 2012, American Society for Microbiology. All Rights Reserved.

doi:10.1128/JB.06105-11

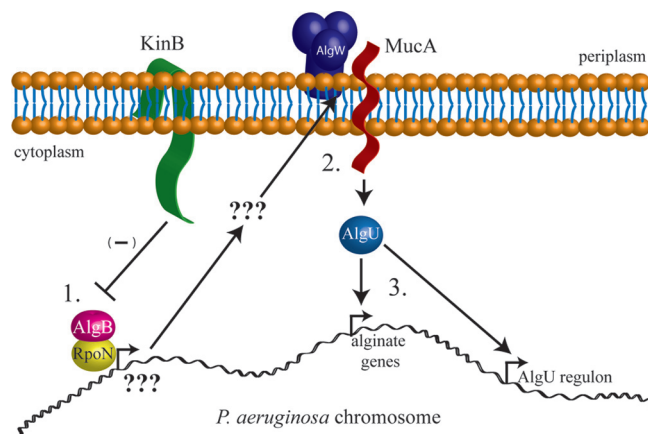


**FIG 1** *P. aeruginosa* sensor kinase KinB regulation of alginate overproduction. KinB is a sensor kinase that localizes to the inner membrane. KinB is also a negative regulator of alginate overproduction (12). We have previously shown that in the absence of *kinB*, AlgB and RpoN activate expression of unknown genes (step 1). These unknown factors caused AlgW-mediated proteolysis of MucA, resulting in activated AlgU (step 2). AlgU then drives expression of the alginate biosynthetic operon as well as other AlgU regulon genes (step 3). The goal of this study is to determine the genes (indicated as ???) controlled by KinB through RpoN.

phosphorylation are mechanisms of signal transduction across the inner membrane and can result in changes in gene expression mediated by the response regulator. *P. aeruginosa* strain PAO1 has 63 sensors and 64 response regulators (47). We recently reported that the inactivation of a gene encoding a histidine kinase, KinB, resulted in alginate overproduction (12). In the PAO1 *kinB* strain, the activated protease AlgW degrades MucA (Fig. 1). Furthermore, regulated proteolysis of MucA is dependent on the cognate response regulator of *kinB*, which is known as AlgB, as well as the *rpoN* gene encoding  $\sigma^{54}$  (12). A CF isolate with the *kinB* mutation has been identified (12). AlgB has been suggested to be an atypical response regulator because AlgB-dependent transcription in alginate regulation does not require phosphorylation (35), and it can be inferred that AlgB would not be phosphorylated in the absence of KinB.

In this study, we analyzed the whole transcriptomes and proteomes of PAO1 *kinB* and PAO1 *kinB*  $\Delta rpoN$  to identify the genes and proteins that are uniquely controlled by KinB and RpoN. Our data indicated that KinB, in concert with RpoN, controls alginate and rhamnolipid expression as well as structural pilus genes and other potentially novel factors. In the *kinB* mutant, RpoN alone represses pyochelin, type IVb pili, antibiotic efflux, and quorum-sensing (QS) genes. In light of these data, we hypothesized that KinB may control virulence in *P. aeruginosa* which was corroborated in an acute murine infection model. Collectively, our data show that KinB is a pleiotropic regulator that through RpoN controls a regulon consisting of approximately 20% of the PAO1 genome and includes the alginate biosynthetic pathway as well as key determinants of virulence.

## MATERIALS AND METHODS

**Bacterial strains and culture medium conditions.** Bacterial strains and plasmids used in this study are indicated in Table S1 in the supplemental material. *P. aeruginosa* strains were grown at 37°C on *Pseudomonas* isolation agar (PIA) plates (Difco). Lysogeny broth (LB)-Miller agar plates

were prepared with 10 g of tryptone, 5 g of NaCl, 10 g of yeast extract, and 15 g of agar per liter.

**RNA isolation and preparation for Affymetrix GeneChip analysis.** *P. aeruginosa* strains were streaked on PIA plates and harvested in a 2:1 solution of phosphate-buffered saline (PBS) and RNA Protect (Qiagen) as per the manufacturer's instructions. After a 10-min incubation at 20°C, cells were centrifuged at  $4,000 \times g$ , and the supernatant was removed. The cell pellet was then resuspended in 1 ml of TRIzol reagent (Invitrogen), and total RNA was purified following the manufacturer's instructions. Total RNA was DNase treated with Ambion's Turbo DNA Free reagent. DNase-treated RNA was used as a template in a 35-cycle PCR to assess the presence of contaminating DNA. RNA quality and the presence of residual DNA were checked on an Agilent Bioanalyzer 2100 electrophoretic system pre- and post-DNase treatment. Ten micrograms of total RNA was used for cDNA synthesis, fragmentation, and labeling according to the Affymetrix GeneChip *P. aeruginosa* genome array expression analysis protocol. Briefly, random hexamers (Invitrogen) were added (final concentration,  $25 \text{ ng } \mu\text{l}^{-1}$ ) to the  $10 \mu\text{g}$  of total RNA along with *in vitro* transcribed *Bacillus subtilis* control spikes (as described in the Affymetrix GeneChip *P. aeruginosa* genome array expression analysis protocol).

cDNA was synthesized using Superscript II (Invitrogen) according to the manufacturer's instructions under the following conditions: 25°C for 10 min, 37°C for 60 min, 42°C for 60 min, and 70°C for 10 min. RNA was removed by alkaline treatment and subsequent neutralization. The cDNA was purified with use of a QIAquick PCR purification kit (Qiagen) and eluted in  $40 \mu\text{l}$  of buffer EB (10 mM Tris-HCl, pH 8.5). The cDNA was fragmented by DNase I ( $0.6 \text{ U } \mu\text{g}^{-1}$  of cDNA; Amersham) at 37°C for 10 min and then end labeled with biotin-ddUTP with use of an Enzo BioArray Terminal Labeling kit (Affymetrix) at 37°C for 60 min. Proper cDNA fragmentation and biotin labeling were determined by gel mobility shift assay with NeutrAvadin (Pierce), followed by electrophoresis through a 5% polyacrylamide gel and subsequent DNA staining with SYBR green I (Roche).

**Microarray data analysis.** Microarray data were generated using Affymetrix protocols as previously described (22, 34, 40, 42). Absolute expression transcript levels were normalized for each chip by globally scaling all probe sets to a target signal intensity of 500. Three statistical algorithms (detection, change call, and signal log ratio) were then used to identify differential gene expression in experimental and control samples. The detection metric (presence, absence, or marginal) for a particular gene was determined using default parameters in MAS software (version 5.0; Affymetrix). Batch analysis was performed in MAS to make pairwise comparisons between individual experimental and control GeneChips in order to generate change calls and a signal log ratio for each transcript. These data were imported into Data Mining Tools (version 3.0; Affymetrix). Transcripts that were absent under both control and experimental conditions were eliminated from further consideration. Statistical significance of signals between the control and experimental conditions ( $P < 0.05$ ) for individual transcripts was determined using the *t* test. We defined a positive change call as one in which greater than 50% of the transcripts had a call of increased (I) or marginally increased (MI) for upregulated genes and decreased (D) or marginally decreased (MD) for downregulated genes. Finally, the mean value of the signal log ratios from each comparison file was calculated. Only those genes that met the above criteria and had a mean signal log ratio of greater than or equal to 1 for upregulated transcripts and less than or equal to 1 for downregulated transcripts were kept in the final list of genes. Signal log ratio values were converted from  $\log_2$  and expressed as fold changes.

**RNA isolation and reverse transcriptase-quantitative PCR (RT-qPCR).** *P. aeruginosa* strains were streaked on PIA plates and harvested in a 2:1 solution of PBS and RNA Protect (Qiagen) as per the manufacturer's instructions. After a 10-min incubation at 20°C, cells were centrifuged at  $4,000 \times g$ , and the supernatant was removed. The cell pellet was then resuspended in 1 ml of TRIzol reagent (Invitrogen), and total RNA was purified following the manufacturer's instructions. Total RNA was DNase

treated with Ambion's Turbo DNA Free reagent. DNase-treated RNA was used as a template in a 35-cycle PCR to assess the presence of contaminating DNA. cDNA samples were generated from 1  $\mu$ g of total RNA using a TaqMan reverse transcription kit (Applied Biosystems) according to the manufacturer's instructions in a total volume of 100  $\mu$ l. Twenty-microliter qPCR mixtures were set up using 1  $\mu$ l of cDNA, 10  $\mu$ l of 2 $\times$  FastStart Universal SYBR green qPCR master mix (Roche), and 4 pmol of each primer (see Table S1 in the supplemental material). qPCRs were performed in 96-well plates in an ABI Prism 7900HT Fast Real Time thermocycler. The program used consisted of an initial 10-min incubation at 95°C, followed by 40 cycles of 15 s at 95°C and 1 min at 60°C. Primer specificity was verified by use of a denaturation step following the last amplification cycle. Threshold cycle ( $C_T$ ) values were collected with a manual threshold of 0.2. Each target was tested in quadruplicate, and the average of the four  $C_T$  values was used for analysis. The average  $C_T$  was converted to a relative transcript number by the equation  $n = 2^{(40 - C_T)}$  as previously described (41). These values were then standardized to the determined value for *omlA*, and the number of target transcripts per *omlA* transcript was calculated. These normalized values were used to determine fold changes.

**Motility assays.** Swimming and swarming assays were performed as described previously (33). Briefly, strains were grown overnight on tryptic soy agar (TSA; Remel) and used to inoculate freshly prepared TSA plates with either 0.4% agar (swimming) or 0.5% agar (swarming). Samples were spotted in triplicate, and the radius of the colony was measured at 24 h postinoculation. Reported values are the average with standard deviation of three replicates. Two methods were employed for twitching motility, subsurface and surface twitching motility assays. Subsurface twitching motility assays were performed as previously described (1). Zones of motility after 48 h of incubation at 37°C were measured after the agar was removed and cells attached to the plastic surface of the petri dish were stained with 0.5%, wt/vol, crystal violet. Surface twitching motility assays were performed as previously described (30, 39). Briefly, buffered twitching motility plates were prepared (10 mM Tris, pH 7.6, 8 mM MgSO<sub>4</sub>, 1 mM NaPO<sub>4</sub>, pH 7.6, and 1.5% agar) and dried for 48 h. Overnight cultures were subcultured, grown to an optical density at 590 nm (OD<sub>590</sub>) of 1.2, and collected by centrifugation to  $9 \times 10^9$  cells/ml in morpholinepropanesulfonic acid (MOPS) buffer (10 mM MOPS, pH 7.6, 8 mM MgSO<sub>4</sub>). A 2.5- $\mu$ l volume of this suspension was placed onto the surface of the agar, and the zone of twitching after 48 h was captured on a Nikon TE2000-U microscope with a 20 $\times$  objective and a DS-Fi1 digital camera (Nikon).

**Rhamnolipid production assay.** Semiquantitative measurements of rhamnolipid production were performed using minimal medium containing cetyl trimethylammonium bromide (CTAB; Acros) and methylene blue (MB; Sigma-Aldrich). Agar plates were made as previously described (43) using 1.6% (vol/vol) glycerol as the sole carbon source. Wells were prepared by pressing a heated 4-mm-diameter glass rod into the agar. Overnight cultures were adjusted by dilution to an OD<sub>600</sub> of 0.2, and 10  $\mu$ l of cultures was inoculated in the wells. Plates were incubated at 37°C for 48 h and subsequently stored at 4°C for 24 h to increase the contrast of the blue halo indicative of surfactant diffusion. Diameters were measured and compared with a standard of known rhamnolipid concentration.

**iTRAQ MALDI-TOF/TOF proteome analysis of PAO1, PAO1 *kinB*, PAO1 *kinB*  $\Delta$ algU, and PAO1 *kinB*  $\Delta$ rpoN.** Strains PAO1, PAO1 *kinB*, PAO1 *kinB*  $\Delta$ algU, and PAO1 *kinB*  $\Delta$ rpoN were cultured on PIA medium for 24 h at 37°C. Total protein samples were prepared using a ProteaPrep Cell Lysis kit, per the manufacturer's instructions. Total protein samples (500  $\mu$ g) were acetone precipitated with a 1:6 dilution and incubated overnight at -20°C. The resulting pellets were reconstituted in 160  $\mu$ l of dissolution buffer for use with isobaric tags for relative and absolute quantification (iTRAQ), to which 8  $\mu$ l of iTRAQ denaturant was added. A total of 16  $\mu$ l of reducing agent was added, and the samples were incubated for 60 min at 60°C. Then, 8  $\mu$ l of cysteine blocking reagent was added, and the samples were incubated for another 10 min in the dark. Trypsin (2  $\mu$ g) was added to the samples for proteolytic degradation, and the reaction was

performed overnight at 37°C. Each sample, PAO1, PAO1 *kinB*, PAO1 *kinB*  $\Delta$ algU, and PAO1 *kinB*  $\Delta$ rpoN, was labeled with iTRAQ reagents 114, 115, 116, and 117, respectively. The labeling of each sample was performed as per the instructions with the kit. The labeling reaction mixture was incubated at room temperature for 60 min. To stop the reactions, 100  $\mu$ l of distilled H<sub>2</sub>O (dH<sub>2</sub>O) was added, and the samples were incubated for 30 min at room temperature. The samples were frozen and then lyophilized. The lyophilized samples were then reconstituted in 50  $\mu$ l of SCX buffer (Protea Biosciences) for fractionation. The samples were transferred to equilibrated SCX ProteaTip Spin Tips and centrifuged at low speed (4,000 rpm) for 2 min. The column was then washed to elute salts and other contaminants with a 50- $\mu$ l rinse solution (5 mM ammonium formate in 10% acetonitrile). The Spin Tip was then added to a clean centrifuge tube, and fractions were collected by 150  $\mu$ l of eight different elution solutions (20, 40, 60, 80, 100, 150, 250, and 500 mM) with 5 mM ammonium formate in 10% acetonitrile. The collected fractions were then cleaned by repeated lyophilization and reconstitution in 0.1 M acetic acid. After final lyophilization, the labeled and digested peptides were reconstituted in 12  $\mu$ l of liquid chromatography buffer (0.1% trifluoroacetic acid [TFA] in water) for liquid chromatography-matrix-assisted laser desorption ionization (LC-MALDI) spotting. An ABI Tempo LC-MALDI instrument was used, running version 2.00.09 software. A Merck Chromolith CapRod monolith column was injected with 10  $\mu$ l of sample. A 30-min separation gradient with two components was used for LC spotting. Buffer A consisted of 0.1% acetic acid and 2% acetonitrile, and buffer B consisted of 0.1% acetic acid and 90% acetonitrile. The ratio of percent A to percent B over the 30-min gradient is available upon request from Protea Biosciences. Spotted samples were then analyzed by an ABI 4800 MALDI-tandem time of flight (TOF/TOF) analyzer with 400 Series Explorer software running acquisition in reflector mode, positive ion mode. A mass range ( $m/z$ ) of 850 to 4,000 was set with 400 laser shots per spectrum. A minimum signal-to-noise ratio of 10 was required for acquisition. Data collected by MALDI-TOF/TOF were then analyzed by ABI ProteinPilot software, version 3.0, using the search engine Paragon with iTRAQ sampling. The ProteinPilot software used the *P. aeruginosa* PAO1 proteome to identify peptides detected in the iTRAQ analysis of the total protein samples. The software reported the number of unique peptides that were found for each protein as well as the percent coverage of the protein. A ratio was derived that compares a peptide from one labeled sample to another labeled sample. If more than one unique peptide was detected and analyzed for a protein, then a *P* value was reported to suggest if the protein is significantly up- or downregulated between the two samples analyzed.

**Murine acute pneumonia model.** *P. aeruginosa* strains were grown on *Pseudomonas* isolation agar (PIA; Becton Dickinson) plates for 24 h at 37°C and suspended in 1 $\times$  PBS to an OD<sub>650</sub> of 1.8. Inocula were diluted 1:1 with 1 $\times$  PBS to obtain the desired challenge dose in 20  $\mu$ l. Six- to 8-week-old female BALB/c mice (Harlan Laboratories) were anesthetized by intraperitoneal injection of 0.2 ml of ketamine (6.7 mg/ml) and xylazine (1.3 mg/ml) in 0.9% saline. Anesthetized animals were placed on their backs, and 10- $\mu$ l inocula were pipetted directly into each nostril (20  $\mu$ l total). Bacterial doses were verified immediately after infection by serial dilution in 1 $\times$  PBS-1% bovine serum albumin (BSA) and plating on PIA. All animals were carefully observed for the duration of the trials. The University of Virginia Animal Care and Use Committee approved all procedures used in this work.

**Microarray data accession number.** The microarray data are available on the GEO (Gene Expression Omnibus) website at <http://www.ncbi.nlm.nih.gov/projects/geo> under accession number GSE35248.

## RESULTS

**Transcriptome analysis of PAO1 *kinB* and PAO1 *kinB*  $\Delta$ rpoN strains.** Typically, wt strains of *P. aeruginosa* such as PAO1 express a nonmucoid phenotype when grown on a common laboratory medium such as PIA. Previous studies established the role of



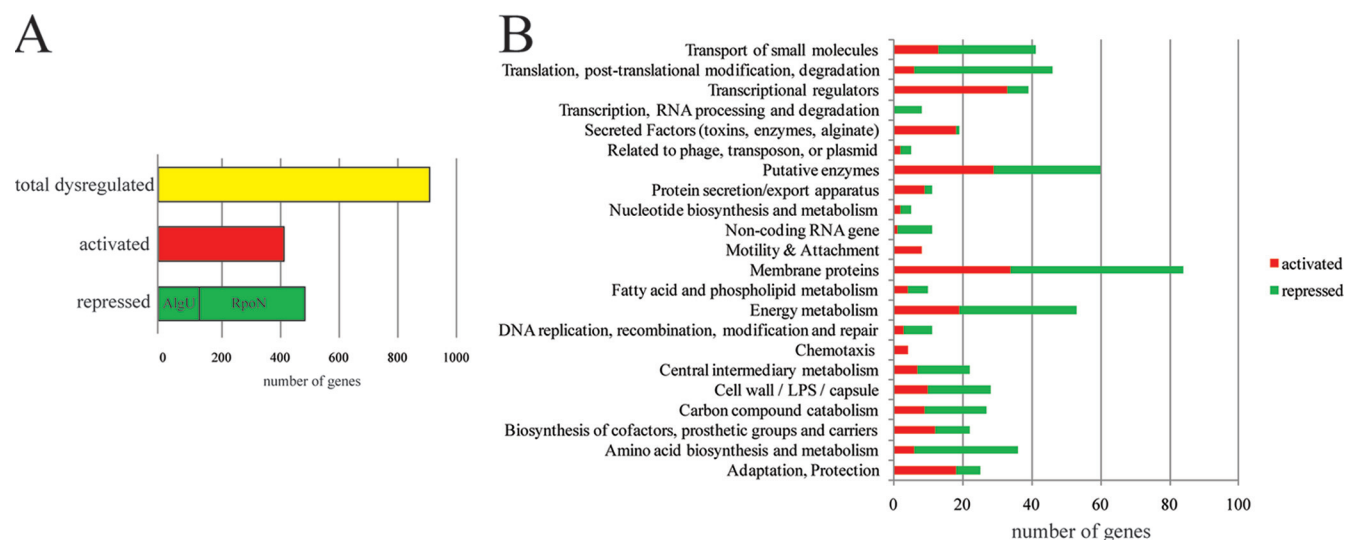


**FIG 2** Microarray analysis of KinB regulon of *P. aeruginosa*. (A) The numbers of genes dysregulated are indicated and subdivided by genes activated (red) and genes repressed (green) due to the deletion of *rpoN* in the *kinB* mutant. Genes which are repressed are further subdivided into those which were previously indicated as AlgU dependent (50), and all others are indicated as RpoN dependent. (B) Genes that were dysregulated were grouped based on their primary PseudoCAP classifications (56). Major classes that were dysregulated between the *kinB* mutant and *kinB rpoN* double mutant are indicated.

MucA, MucB, and MucD as negative alginate regulators (4, 24, 36). We recently showed that the inactivation or deletion of *kinB* caused AlgW-mediated proteolysis of MucA, which also results in alginate overproduction (12). Interestingly, in the *kinB* mutant, AlgU activity and MucA degradation required the transcriptional regulator AlgB and alternate sigma factor RpoN (12). From these data a proteolysis-mediated model of alginate regulation was proposed where AlgB and RpoN control the expression of factors that can activate AlgW to degrade MucA. Therefore, the loss of *rpoN* would cause a decrease in the expression of alginate synthesis genes due to the lowered AlgU activity (Fig. 1). The effect of AlgB on the *P. aeruginosa* transcriptome, as has been previously shown (32), is through binding to *PalgD* to activate transcription of the alginate biosynthetic operon. In order to understand the effect of the *kinB* and *rpoN* mutations on the transcriptome, microarray analysis was performed on the mucoid *kinB* mutant, and data were compared to results of the nonmucoid *kinB rpoN* double mutant. To our surprise, a vast number of genes (926 genes) were dysregulated due to deletion of *rpoN* in the *kinB* mutant (Fig. 2A and Tables 1 and 2; see also Table S2 in the supplemental material). Previous microarray analysis indicated that the loss of *rpoN* caused the dysregulation of 62 genes in *P. aeruginosa* strain PAK (14). Here, we observed that the KinB-RpoN regulon is made up of 926 genes, which represent approximately 20% of the PAO1 genome (see Table S2). Of these 926 genes, 499 were repressed, and 427 were activated (Fig. 2A). Seventeen of the 62 previously reported dysregulated genes due to loss of *rpoN* were confirmed (see Table S2). Since the *kinB* strain is mucoid and has high AlgU activity (12), we expected to observe genes in the KinB regulon that were dependent on AlgU. Multiple transcriptome studies have been performed with *mucA* mutants (18–21) and compounds that activate regulated proteolysis of MucA (57, 59). We chose to define genes as AlgU dependent based on an analysis by Tart et al. (50), which utilized an isogenic *algU* pair to define the AlgU regulon. We observed that 139 AlgU-dependent genes (50) were also downregulated in the PAO1 *kinB ΔrpoN* strain, con-

firmed our previous hypothesis that RpoN regulates AlgU activity. Interestingly, we observed 360 genes that were dependent on RpoN and that had not been found to be AlgU regulated (Fig. 2A; see also Table S2 in the supplemental material).

KinB-RpoN regulon genes were grouped by PseudoCAP class (56) and plotted with respect to activation or repression in Fig. 2B. A large number of hypothetical genes were dysregulated but are not indicated in Fig. 2B. A total of 182 hypothetical genes were activated, and 155 hypothetical genes were repressed when the *kinB rpoN* double mutant was compared to the *kinB* strain. In the *kinB* mutant, deletion of *rpoN* caused activation of 18 genes in the adaptation and protection class but also repressed 7 genes (Fig. 2B). Of particular interest, 30 genes involved in amino acid biosynthesis and metabolism were repressed due to the deletion of *rpoN* in the *kinB* mutant. Eighteen genes encoding secreted factors were activated in the *kinB rpoN* double mutant (Fig. 2B). We also observed that genes encoding 34 membrane proteins were activated, and 50 were repressed due to the *rpoN* deletion in the *kinB* background. These data support the hypothesis that a connection between RpoN and outer membrane protein expression exists. Similarly, a large number of genes which encode proteins that function in small-molecule transport were repressed in the *kinB rpoN* double mutant (Fig. 2B).

**AlgW expression in the *kinB* and *kinB ΔrpoN* mutants.** In our previous study, MucA degradation in the *kinB* mutant was abrogated by the deletion of *rpoN* (12). We hypothesized that this may be due to the loss of AlgW protease activity or the absence of an unknown factor (12). Transcriptome analysis showed that the expression of *algW* decreased by 11-fold in the PAO1 *kinB ΔrpoN* strain compared to PAO1 *kinB* (Table 1). To validate this, reverse transcriptase quantitative PCR (RT-qPCR) was performed and showed that *algW* expression was 2.9-fold lower in the PAO1 *kinB ΔrpoN* mutant than in the PAO1 *kinB* strain (Table 3). PAO1 also showed less AlgW expression than PAO1 *kinB* under the same conditions (Table 3). These data suggest that AlgW expression is affected by RpoN and KinB, which supports our previously pro-

TABLE 1 KinB regulon genes with decreased expression due to *rpoN* deletion

Gene group and PA locus	Gene	Product	Fold change	Sigma dependence <sup>a</sup>
Alginate and related genes				
PA0762	<i>algU</i>	Sigma factor AlgU	NS <sup>c</sup>	RpoN, AlgU
PA0763	<i>mucA</i>	Anti-sigma factor MucA	NS	RpoN, AlgU
PA0764	<i>mucB</i>	Negative regulator for alginate biosynthesis MucB	−2.8	RpoN, AlgU
PA0765	<i>mucC</i>	Positive regulator for alginate biosynthesis MucC	−2.3	RpoN, AlgU
PA0766	<i>mucD</i>	Serine protease MucD precursor	−2.8	RpoN, AlgU
PA3540	<i>algD</i>	GDP-mannose 6-dehydrogenase AlgD	−71.6	RpoN, AlgU
PA3541	<i>alg8</i>	Alginate biosynthesis protein Alg8	−13.9	RpoN, AlgU
PA3542	<i>alg44</i>	Alginate biosynthesis protein Alg44	−13.0	RpoN, AlgU
PA3543	<i>algK</i>	Alginate biosynthetic protein AlgK precursor	−16.5	RpoN, AlgU
PA3544	<i>algE</i>	Alginate production outer membrane protein AlgE	−13.8	RpoN, AlgU
PA3545	<i>algG</i>	Alginate-c5-mannuronan-epimerase AlgG	−12.6	RpoN, AlgU
PA3546	<i>algX</i>	Alginate biosynthesis protein AlgX	−12.9	RpoN, AlgU
PA3547	<i>algL</i>	Poly(beta-D-mannuronate) lyase precursor AlgL	−20.2	RpoN, AlgU
PA3548	<i>algI</i>	Alginate O-acetyltransferase AlgI	−13.7	RpoN, AlgU
PA3549	<i>algJ</i>	Alginate O-acetyltransferase AlgJ	−15.0	RpoN, AlgU
PA3550	<i>algF</i>	Alginate O-acetyltransferase AlgF	−25.0	RpoN, AlgU
PA3551	<i>algA</i>	Phosphomannose isomerase/guanosine 5'-diphospho-D-mannose pyrophosphorylase	−46.8	RpoN, AlgU
PA4446	<i>algW</i>	Regulated protease AlgW	−11.1	RpoN
PA5322	<i>algC</i>	Phosphomannomutase AlgC	−4.5	RpoN, AlgU
PA5483	<i>algB</i>	Two-component response regulator AlgB	−3.0	RpoN, AlgU
PA3692	<i>lptF</i>	Lipotoxin F, LptF	−5.9	RpoN, AlgU
PA21XX metabolic operon genes				
PA2134		Hypothetical protein	−14.6	RpoN
PA2135		Probable transporter	−4.4	RpoN
PA2136		Hypothetical protein	−2.2	RpoN
PA2137		Hypothetical protein	−4.3	RpoN
PA2138		Probable ATP-dependent DNA ligase	−3.3	RpoN
PA2139		Hypothetical protein	−3.8	RpoN
PA2140		Probable metallothionein	−2.8	RpoN
PA2141		Hypothetical protein	−3.9	RpoN
PA2142	<i>yhxC</i>	Probable short-chain dehydrogenase	−3.7	RpoN
PA2143		Hypothetical protein	−16.1	RpoN
PA2144	<i>glgP</i>	Glycogen phosphorylase	−8.2	RpoN
PA2145		Hypothetical protein	−4.6	RpoN
PA2146		Conserved hypothetical protein	−4.2	RpoN, AlgU
PA2147	<i>katE</i>	Catalase HP11	−34.3	RpoN, AlgU
PA2148		Conserved hypothetical protein	−7.6	RpoN
PA2149		Hypothetical protein	−10.3	RpoN
PA2150		Conserved hypothetical protein	−8.5	RpoN
PA2151		Conserved hypothetical protein	−10.6	RpoN
PA2152		Probable trehalose synthase	−8.8	RpoN
PA2153	<i>glgB</i>	1,4-Alpha-glucan branching enzyme	−10.2	RpoN
PA2154	<i>ybhN</i>	Conserved hypothetical protein	−4.4	RpoN
PA2155	<i>ybhO</i>	Probable phospholipase	−6.7	RpoN
PA2156	<i>ybhP</i>	Conserved hypothetical protein	−5.9	RpoN
PA2157		Hypothetical protein	−5.2	RpoN
PA2158		Probable alcohol dehydrogenase (Zn dependent)	−10.3	RpoN
PA2159		Conserved hypothetical protein	−13.3	RpoN
PA2160	<i>glgX</i>	Probable glycosyl hydrolase	−14.8	RpoN
PA2161		Hypothetical protein	−14.3	RpoN, AlgU <sup>b</sup>
PA2162		Probable glycosyl hydrolase	−9.5	RpoN
PA2163		Hypothetical protein	−10.6	RpoN
PA2164		Probable glycosyl hydrolase	−14.1	RpoN
PA2165	<i>glgA</i>	Probable glycogen synthase	−10.5	RpoN, AlgU
PA2167		Hypothetical protein	−2.6	RpoN <sup>b</sup>
PA2168		Hypothetical protein	−2.5	RpoN
PA2169		Hypothetical protein	−20.9	RpoN

(Continued on following page)

TABLE 1 (Continued)

Gene group and PA locus	Gene	Product	Fold change	Sigma dependence <sup>a</sup>
PA2170		Hypothetical protein	−40.3	RpoN, AlgU
PA2171		Hypothetical protein	−13.9	RpoN, AlgU
PA2172		Hypothetical protein	−23.1	RpoN, AlgU <sup>b</sup>
PA2173		Hypothetical protein	−16.4	RpoN, AlgU
PA2175		Hypothetical protein	−4.9	RpoN
PA2176		Hypothetical protein	−4.2	RpoN, AlgU
PA2178		Hypothetical protein	−5.7	RpoN
PA2179		Hypothetical protein	−8.8	RpoN
PA2180		Hypothetical protein	−16.0	RpoN
PA2181		Hypothetical protein	−4.9	RpoN
PA2182		Hypothetical protein	−2.6	RpoN
PA2183		Hypothetical protein	−7.5	RpoN
PA2184	<i>yciE</i>	Conserved hypothetical protein	−18.7	RpoN
PA2185	<i>katN</i>	Nonheme catalase KatN	−9.7	RpoN
PA2186		Hypothetical protein	−3.1	RpoN
PA2187		Hypothetical protein	−10.7	RpoN
PA2188		Probable alcohol dehydrogenase (Zn dependent)	−3.5	RpoN
PA2190		Conserved hypothetical protein	−3.0	RpoN
PA2192		Conserved hypothetical protein	−9.3	RpoN
Other genes				
PA2416	<i>treA</i>	Periplasmic trehalase precursor	−7.1	RpoN
PA1471		Extracellular hypothetical	−31.7	RpoN
PA4880		Probable bacterioferritin	−16.1	RpoN, AlgU
PA4171		Probable cytoplasmic protease	−11.8	RpoN
PA0985		Pyocin S5	−5.0	RpoN
PA0355		Cytoplasmic protease PfpI	−5.0	RpoN, AlgU
PA5119	<i>glnA</i>	Glutamine synthetase	−2.6	RpoN
PA0298	<i>spuB</i>	Probable glutamine synthetase	−2.5	RpoN, AlgU

<sup>a</sup> Sigma factor dependence was determined by selecting all genes downregulated and then filtering genes that were either dependent on AlgU (as ascertained by Tart et al. [50]) and RpoN or only RpoN.

<sup>b</sup> Wu et al. (61) indicated that these genes are upregulated in strain PAK *mucA22* and are therefore AlgU dependent.

<sup>c</sup> NS, nonsignificant.

posed hypothesis that RpoN may affect the AlgW protease activity and/or expression.

**KinB and RpoN control expression of alginate biosynthetic genes and genes associated with carbohydrate metabolism.** Comparison of the PAO1 *kinB* and PAO1 *kinB*  $\Delta$ *rpoN* transcriptomes indicated that alginate biosynthetic gene expression was significantly lower in PAO1 *kinB*  $\Delta$ *rpoN*, as would be expected in any comparison between a mucoid and a nonmucoid strain (Table 1). Since AlgU activity in PAO1 *kinB* depends on RpoN (12), it is not surprising to see that many AlgU-dependent genes are also dependent on RpoN in PAO1 *kinB* (Table 1). Interestingly, *algW* was the only alginate gene detected that is only RpoN dependent and not dependent on both RpoN and AlgU. These data suggest a hierarchy of alginate gene expression where RpoN controls regulatory elements such as AlgW that can activate the AlgU pathway leading to alginate synthesis. In the transcriptome analysis (Table 1), no significant changes in *algU* and *mucA* expression were observed between PAO1 *kinB* and PAO1 *kinB*  $\Delta$ *rpoN* strains. However, RT-qPCR showed that *algU* and *mucA* expression levels decreased 10.5- and 8.8-fold, respectively, due to loss of *rpoN* (Table 3), as was previously shown (12).

Examination of the RpoN-dependent genes in a *kinB* background revealed a chromosomal region from PA2134 to PA2192 comprised of 54 genes whose expression was dependent on RpoN in PAO1 *kinB* (Table 1). Other investigators have noticed that this

same chromosomal region was differentially expressed in planktonic and biofilm stationary-phase growth transcriptomes (53). In our study, all of these genes were dependent on RpoN. Here, this region of genes will be referred to as the PA21XX region. Interestingly, in mucoid strains, a subset of these genes in the middle of this chromosomal region were previously shown to be regulated by AlgU (PA2146, PA2147, PA2161, PA2165, PA2170, PA2171, PA2172, PA2173, and PA2176) (50) (Table 1). Three of these genes (PA2161, PA2167, and PA2172) have been shown to be AlgU dependent (61).

**iTRAQ analysis of the *kinB* mutant proteome.** While transcriptome analysis provided new insights into the effect of the loss of *kinB*, we sought to further characterize the effect by examining the proteome of *P. aeruginosa* strains PAO1, PAO1 *kinB*, PAO1 *kinB*  $\Delta$ *algU*, and PAO1 *kinB*  $\Delta$ *rpoN* by using isobaric tags for relative and absolute quantification (iTRAQ). iTRAQ uses the analysis of MALDI-TOF (matrix-assisted laser desorption ionization–time of flight) mass spectrometry (MS) with tagged peptides that allow multiple protein samples to be examined and the relative quantity of proteins to be measured. Our data for iTRAQ analysis of the strains are shown in Table 4 and Table S3 in the supplemental material. A total of 1,448 peptides that had 95% confidence values were observed in the four-sample multiplex, and of these, 740 were distinct and corresponded to 121 proteins to which relative intensity and *P* values could be assigned. Similar

TABLE 2 KinB regulon genes with increased expression due to *rpoN* deletion

Gene group and PA locus	Gene	Product	Fold change <sup>a</sup>
Pyochelin genes			
PA4220	<i>fptB</i>	Hypothetical protein	25.1
PA4221	<i>fptA</i>	Fe(III)-pyochelin outer membrane receptor precursor	7.1
PA4222	<i>pchI</i>	Probable ATP-binding component of ABC transporter	14.3
PA4223	<i>pchH</i>	Probable ATP-binding component of ABC transporter	11.7
PA4224	<i>pchG</i>	Pyochelin biosynthetic protein PchG	21.3
PA4225	<i>pchF</i>	Pyochelin synthetase	13.2
PA4226	<i>pchE</i>	Dihydroaeruginic acid synthetase	16.8
PA4227	<i>pchR</i>	Transcriptional regulator PchR	2.2
PA4228	<i>pchD</i>	Pyochelin biosynthesis protein PchD	7.7
PA4229	<i>pchC</i>	Pyochelin biosynthetic protein PchC	5.3
PA4230	<i>pchB</i>	Salicylate biosynthesis protein PchB	25.5
PA4231	<i>pchA</i>	Salicylate biosynthesis isochorismate synthase	12.2
Pilus genes			
PA4651	<i>cupE4</i>	Pilin assembly chaperone CupE4	19.8
PA4293	<i>pprA</i>	Probable pili assembly chaperone	12.5
PA4294		Hypothetical protein	12.1
PA4296	<i>pprB</i>	Two-component response regulator, PprB	3.5
PA4297	<i>tadG</i>	TadG	2.7
PA4298		Hypothetical protein	5.0
PA4299	<i>tadD</i>	TadD	13.1
PA4300	<i>tadC</i>	TadC	7.4
PA4301	<i>tadB</i>	TadB	5.9
PA4302	<i>tadA</i>	TadA ATPase	5.0
PA4303	<i>tadZ</i>	TadZ	7.1
PA4304	<i>rcpA</i>	RcpA	11.7
PA4305	<i>rcpC</i>	RcpC	13.4
PA4306	<i>flp</i>	Type IVb pilin, Flp	26.1
Antibiotic efflux genes			
PA1874		Hypothetical protein	14.8
PA1875	<i>opmL</i>	Probable outer membrane protein precursor	19.5
PA1876		Probable ATP-binding/permease fusion ABC transporter	8.3
PA1877	<i>hlyD</i>	Probable secretion protein	5.0
PA4293	<i>pprA</i>	Two-component sensor kinase PprA	12.5
PA4294	<i>pprB</i>	Response regulator PprB	12.1
PA4205	<i>mexG</i>	Hypothetical protein	8.5
PA4206	<i>mexH</i>	Probable efflux membrane fusion protein precursor	7.4
PA4207	<i>mexI</i>	Probable efflux transporter	4.9
PA4208	<i>opmD</i>	Probable outer membrane protein precursor	5.1
PA4218	<i>ampP</i>	AmpP $\beta$ -lactamase permease	6.1
PA4219	<i>ampO</i>	AmpO	12.0
Quorum-sensing genes			
PA3622	<i>rpoS</i>	Sigma factor RpoS	NS
PA1430	<i>lasR</i>	Transcriptional regulator LasR	NS
PA1432	<i>lasI</i>	Autoinducer synthesis protein LasI	NS
PA1871	<i>lasA</i>	LasA protease precursor	12.0
PA3724	<i>lasB</i>	Elastase LasB	3.2
PA3476	<i>rhII</i>	Autoinducer synthesis protein RhII	3.3
PA3477	<i>rhIR</i>	Transcriptional regulator RhIR	NS
PA3478	<i>rhIB</i>	Rhamnosyltransferase chain B	10.0
PA3479	<i>rhIA</i>	Rhamnosyltransferase chain A	10.7
PA1245		Hypothetical protein	2.8
PA1246	<i>aprD</i>	Alkaline protease secretion protein AprD	3.5
PA1247	<i>aprE</i>	Alkaline protease secretion protein AprE	3.6
PA1248	<i>aprF</i>	Alkaline protease secretion outer membrane protein AprF	2.6
PA1249	<i>aprA</i>	Alkaline metalloproteinase precursor	NS

(Continued on following page)

TABLE 2 (Continued)

Gene group and PA locus	Gene	Product	Fold change <sup>a</sup>
Nitrogen regulation genes			
PA0518	<i>nirM</i>	Cytochrome c551 precursor	2.3
PA0519	<i>nirS</i>	Nitrite reductase precursor	2.8
PA0520	<i>nirQ</i>	Regulatory protein NirQ	4.0
PA0523	<i>norC</i>	Nitric-oxide reductase subunit C	5.1
PA0524	<i>norB</i>	Nitric-oxide reductase subunit B	2.6
PA0525	<i>norD</i>	Probable dinitrification protein NorD	6.1
PA3391	<i>nosR</i>	Regulatory protein NosR	2.6
Other genes and virulence factors			
PA2300	<i>chiC</i>	Chitinase	16.2
PA2570	<i>lecA</i>	LecA PA-I galactophilic lectin	16.1
PA2788		Probable chemotaxis transducer	14.7
PA4351		Probable acyltransferase	14.0
PA3126	<i>lbpA</i>	Heat shock protein lbpA	7.1

<sup>a</sup> NS, nonsignificant.

to the transcriptome analyses, PA2169, PA2171, PA2184, and PA2190 were upregulated in the *kinB* mutant (Table 4) and repressed in the PAO1 *kinB*  $\Delta$ *rpoN* strain. However, we could determine that only PA2184 and PA2190 were upregulated to a statistically significant level (see Table S3 in the supplemental material), but PA2169 and PA2171 were not significantly upregulated. The most plausible explanation is that since a distinct tryptic peptide must be found in each sample, some proteins will lack enough trypsin recognition sites. However, our analysis of the *kinB* mutant as well as PAO1 *kinB*  $\Delta$ *algU* and PAO1 *kinB*  $\Delta$ *rpoN* mutants supported the transcriptome analysis and suggests that the PA21XX chromosomal region is controlled by RpoN and KinB and may play a role in metabolic pathways.

TABLE 3 RT-qPCR analysis of KinB-RpoN regulon genes

Gene or ORF	Product	Fold change	
		PAO1 <i>kinB</i> $\Delta$ <i>rpoN</i> vs PAO1 <i>kinB</i>	PAO1 vs PAO1 <i>kinB</i>
<i>algU</i>	Sigma factor AlgU	−10.5	1.1
<i>mucA</i>	Anti-sigma factor MucA	−8.8	1.3
<i>algW</i>	Regulated protease AlgW	−2.9	−1.5
PA2146	Conserved hypothetical protein	−11,701.6	−74.7
<i>katE</i>	Catalase HPII	−6.2	−2.5
<i>treA</i>	Periplasmic trehalase precursor	−11.7	1.4
PA1471	Extracellular hypothetical	−125.9	−31.8
<i>pchA</i>	Salicylate biosynthesis isochorismate synthase	−2.2	−27.0
<i>pchG</i>	Pyochelin biosynthesis protein PchG	3.2	57.7
<i>fptA</i>	Fe(III)-pyochelin outer membrane receptor	2.2	25.5
<i>lecA</i>	LecA PA-I galactophilic lectin	6.2	472.3
<i>aprA</i>	Alkaline metalloproteinase precursor	12.0	34.6
<i>aprD</i>	Alkaline protease secretion protein AprD	14.4	28.7
<i>rhIA</i>	Rhamnosyltransferase chain A	5.7	29.8
<i>rhIB</i>	Rhamnosyltransferase chain B	27.8	114.4
<i>rhII</i>	Autoinducer synthesis protein RhII	7.7	21.2
<i>lasB</i>	Elastase LasB	2.0	180.7
<i>lasI</i>	Autoinducer synthesis protein LasI	1.2	1.8

**RpoN negatively regulates pyochelin synthesis.** Transcriptome analysis of nonmucoid strain PAO1 *kinB*  $\Delta$ *rpoN* strain revealed that the entire pyochelin biosynthetic operon was upregulated compared to the level in the mucoid PAO1 *kinB* (Table 2). Pyochelin is one of the iron siderophores *P. aeruginosa* uses to scavenge iron from the environment. Fold changes of 7.1, 21.3, and 12.2 were observed for pyochelin genes *fptA*, *pchG*, and *pchA*, respectively (Table 2). RT-qPCR was utilized to validate these gene expression changes because proteomic analysis failed to detect the biosynthetic enzymes. As shown in Table 3, RT-qPCR indicated fold changes of −2.2, −3.2, and −2.2 for *fptA*, *pchG*, and *pchA*, respectively. Our data suggest that *rpoN* may be a negative regulator of pyochelin biosynthesis gene expression in the mucoid PAO1 *kinB* mutant.

**KinB and RpoN regulation of motility.** RpoN positively regulates both flagella (52) and type IVa pili (29) in *P. aeruginosa*. Furthermore, AlgU has been shown to repress both flagella (50) and pili (3). However, in the *kinB* mutant, increased type IVb pilus gene expression was observed when *rpoN* was absent (Table 2). Multiple distinct genetic systems contribute to overall cellular motility of *P. aeruginosa*. To ascertain the effects of the *rpoN* deletion in the *kinB* mutant, motility assays measuring swimming, swarming, and twitching were performed. Using 0.3%, 0.5%, and 1% agar, respectively, swimming, swarming, and twitching were measured, and results are indicated in Fig. 3A. Both surface and subsurface twitching motility assays were performed to assess type IV pilus functionality (1, 39). The *kinB* mutation decreased all three forms of motility. Not surprisingly, *rpoN* deletion completely abrogated swimming and twitching motility; however, a small amount of swarming was observed in the *kinB*  $\Delta$ *rpoN* strain (Fig. 3A and B). Interestingly, deletion of *algU* restored the *kinB* mutant back to wild-type levels of swimming and swarming but not twitching motility (Fig. 3A).

**Quorum-sensing gene systems are negatively controlled by RpoN in the *kinB* mutant.** *P. aeruginosa* has an elaborate quorum-sensing (QS) system utilizing three autoinducer molecules. *N*-3-Oxododecanoyl-homoserine lactone (3OC12-HSL) is produced by LasI (55), and at the threshold concentration, enough 3OC12-HSL binds to LasR to allow for population-wide transcriptional activation (55). Upon dimerization of LasR, ex-



TABLE 4 iTRAQ quantitative proteomic analysis of strains PAO1, PAO1 *kinB*, PAO1 *kinB*  $\Delta$ *algU*, and PAO1 *kinB*  $\Delta$ *rpoN*

Locus	Name	PseudoCAP functional class	Fold change		
			PAO1 <i>kinB</i> vs PAO1	PAO1 <i>kinB</i> $\Delta$ <i>algU</i> vs PAO1 <i>kinB</i>	PAO1 <i>kinB</i> $\Delta$ <i>rpoN</i> vs PAO1 <i>kinB</i>
PA2146	Conserved hypothetical protein	Hypothetical, unclassified, unknown	16.47	−22.90	−23.33
PA2169	Hypothetical protein	Hypothetical, unclassified, unknown	−0.52	−1.99	−1.99
PA2171	Hypothetical protein	Hypothetical, unclassified, unknown	2.38	−2.04	−1.77
PA2184	Conserved hypothetical protein	Hypothetical, unclassified, unknown	2.32	−3.91	−3.02
PA2190	Conserved hypothetical protein	Hypothetical, unclassified, unknown	2.02	−3.37	−2.08
PA3309	Conserved hypothetical protein	Hypothetical, unclassified, unknown	−1.86	1.67	1.76
PA4739	Conserved hypothetical protein	Hypothetical, unclassified, unknown	5.00	−3.96	−1.43
PA5339	Conserved hypothetical protein	Hypothetical, unclassified, unknown	−1.33	1.36	1.55
PA5481	Hypothetical protein	Hypothetical, unclassified, unknown	5.08	−3.52	−3.10
PA4251	50S Ribosomal protein L5	Translation, modification, degradation	−1.67	1.24	1.70
PA4277	Elongation factor Tu	Translation, modification, degradation	−1.17	1.19	1.34
PA4922	Azurin precursor	Energy metabolism	−1.15	1.19	1.31
PA5556	ATP synthase alpha chain	Energy metabolism	−1.33	1.12	1.36
PA2300	Chitinase	Carbon compound catabolism	−1.82	2.04	2.20
PA4385	GroEL protein	Chaperones and heat shock proteins	−2.02	1.32	1.83
PA4761	DnaK protein	Heat shock proteins	1.10	−1.15	1.11
PA0766	Serine protease MucD	Toxins, enzymes, alginate	−1.24	−1.72	−0.87
PA1342	ABC transporter	Transport of small molecules	−1.53	1.17	1.43
PA0888	Binding protein AotJ	Transport of small molecules	−1.69	1.81	2.13
PA1092	Flagellin type B	Motility and attachment	−2.20	2.04	2.28
PA1159	Probable cold shock protein	Transcriptional regulators	−1.22	−1.00	1.19
PA0456	Probable cold shock protein	Transcriptional regulators	−0.81	−1.51	−1.16
PA4315	Transcriptional regulator MvaT	Transcriptional regulators	−0.73	−1.65	−1.44
PA0852	Chitin-binding protein CbpD	Toxins, enzymes, alginate	−1.25	1.42	1.26
PA4238	DNA-directed RNA polymerase	Transcription, processing and degradation	1.00	−1.34	1.03
PA5171	Arginine deiminase	Amino acid biosynthesis and metabolism	−1.74	1.38	1.39

pression of QS genes will occur (15). However, no significant change in either *lasI* or *lasR* expression was observed in the transcriptome analysis (Table 2). Previously, we noted a high number of QS-regulated proteins identified in the *kinB* mutant (11). The transcriptome analysis revealed a large number of QS-regulated genes with increased expression levels in the PAO1 *kinB*  $\Delta$ *rpoN* strain (Table 2). The expression levels of *rhlI* were increased in the PAO1 *kinB*  $\Delta$ *rpoN* strain (Tables 2 and 3). This suggests that the increased expression of QS genes may be due to the second class of *P. aeruginosa* QS molecules, *N*-butyryl-homoserine lactone (C4-HSL). A number of genes that are controlled by both 3OC12-HSL and C4-HSL (49) also showed increased expression levels in the PAO1 *kinB*  $\Delta$ *rpoN* strain (Table 2). Therefore, it is difficult to determine which QS signal is responsible for increased QS-dependent gene expression. QS-controlled *lasB*, which encodes the LasB protease, was increased 3-fold in the transcriptome analysis and 2-fold by RT-qPCR. Furthermore, the rhamnolipid genes *rhlA* and *rhlB* were 10-fold upregulated in PAO1 *kinB*  $\Delta$ *rpoN* in the transcriptome analysis (Table 2) and 7.7 and 27.8, respectively, by RT-qPCR (Table 3). PAO1 and PAO1 *kinB*  $\Delta$ *rpoN* produced three times more rhamnolipids than PAO1 *kinB*, indicating that RpoN repressed this product of the Rhl quorum-sensing system (Fig. 4A and B). The increased levels of rhamnolipid production may explain the residual swarming observed in the PAO1 *kinB*  $\Delta$ *rpoN* mutant (Fig. 3A). The discrepancy between the measured amounts of rhamnolipids and the transcription of *rhlAB* are likely due to posttranscriptional regulation by other factors such as the small noncoding RNA binding protein RsmA (28). Other QS-regulated genes were noted in our transcriptome analysis. Alkaline

protease operon *apr-aprF* was upregulated, yet *aprA* encoding alkaline protease was not significantly upregulated in the transcriptome (Table 2). However, RT-qPCR revealed that *aprA* was 12-fold upregulated in PAO1 *kinB*  $\Delta$ *rpoN* over PAO1 *kinB* (Table 3). The third class of QS inducers, *Pseudomonas* quinolone signal (PQS), were not dysregulated by the *kinB* mutation or the combination of the *kinB* and *rpoN* mutations. Collectively, our microarray analysis and RT-qPCR data suggest that *rpoN* may repress the Rhl system in the *kinB* mutant.

**KinB, RpoN, and AlgU control virulence of *P. aeruginosa* in a murine model.** Our transcriptomic, proteomic, and phenotypic analyses of the mucoid PAO1 *kinB* strain and nonmucoid PAO1 *kinB*  $\Delta$ *rpoN* double mutant showed that KinB controls not only alginate but also a wide array of genes and virulence factors. Since sensor kinases monitor the environment and activate responses, KinB may be required for virulence. Furthermore, other investigators have shown that *kinB* is required for virulence in a zebra fish model (7). To test this hypothesis, an acute pneumonia model was utilized with BALB/c mice infected by the intranasal route. Since the *kinB* mutant is mucoid, PDO300, a mucoid *mucA22* mutant (37) with a wild-type *kinB*, was used for comparison. With a dose of  $1 \times 10^7$  CFU of bacteria, 0% of BALB/c mice survived infection by PAO1 after 40 to 50 h (Fig. 5). Similar mortality was observed with mucoid strain PDO300 (Fig. 5). However, PAO1 *kinB* did not cause the death of any mice (Fig. 5). PAO1 *kinB*  $\Delta$ *rpoN* caused slightly greater mortality than PAO1 *kinB*; however, 75% of the mice survived the infection (Fig. 5). Interestingly, nonmucoid PAO1 *kinB*  $\Delta$ *algU* caused a similar rate of mortality as PAO1 (Fig. 5). Collectively, these data suggest that KinB/RpoN regulates vir-

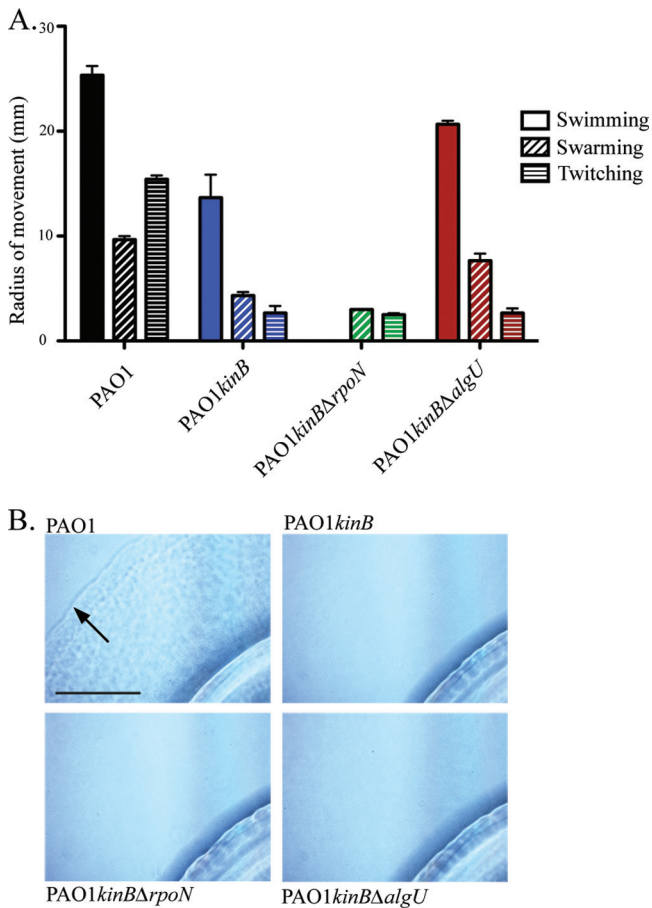


**FIG 3** Motility of *P. aeruginosa* *kinB* mutant strains. (A) Swimming, swarming, and twitching motility are shown for the strain indicated, with standard deviations. (B) Representative surface twitching motility. Cultures adjusted to an  $A_{590}$  of 1.2 were centrifuged and resuspended in MOPS buffer, and 2.5  $\mu$ l was spotted onto the surface of a predried buffered agar plate, as described in Materials and Methods. Organisms were allowed to twitch outwards for 48 h at 37°C. The arrow shows the leading edge of PAO1 twitching ( $n = 3$ ). Bar, 500  $\mu$ m.

ulence factors and may be required for virulence in acute infection by *P. aeruginosa*.

**DISCUSSION**

Our data suggest that KinB negatively regulates alginate overproduction due to *algW* expression. Furthermore, KinB and RpoN may regulate the carbon flux from carbohydrate metabolism. We anticipated and found that the expression of the alginate biosynthetic operon was decreased in the *kinB*  $\Delta$ *rpoN* double mutant; however, we did not expect the downregulation of a 54-gene chromosomal region, PA21XX (PA2134 to PA2192) (Table 1). It seems probable that the chromosomal region PA21XX is responsible for carbohydrate metabolism. RpoN has been inactivated from *mucA* mucoid mutants before by our laboratory (unpublished results) and by others (52), and no change in the mucoid phenotype was observed. However, the *kinB* mutant (12) and the unidentified *muc*-23 mutant PAO579 require *rpoN* for alginate production (5). One observation that may help to explain the differences between *mucA* strains and wt strains is that the PA21XX chromosomal region

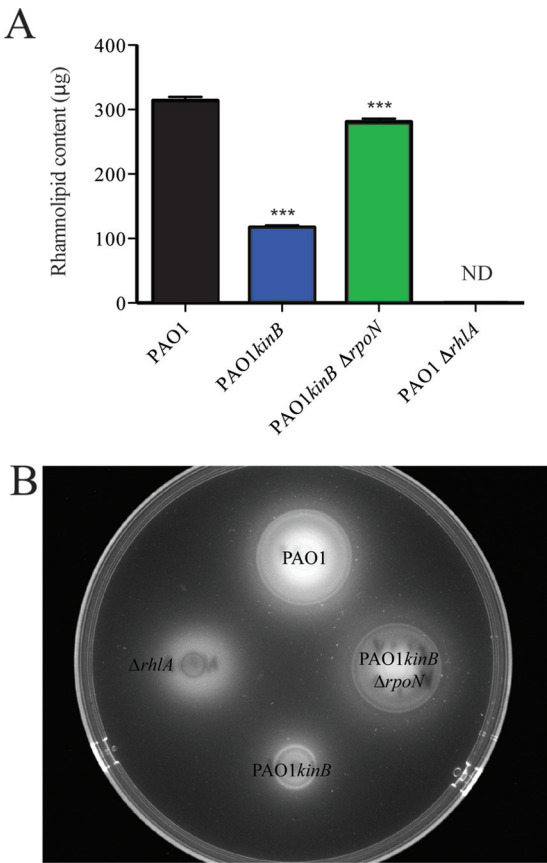


**FIG 4** Rhamnolipid production of *P. aeruginosa* PAO1, *kinB*, and *kinB*  $\Delta$ *rpoN* strains. (A) Rhamnolipid content is shown for the strains indicated, with PAO1  $\Delta$ *rhlA* as a negative control. ND, statistical analysis was not determined due to the values of 0. \*\*\*, significant *P* values compared to PAO1. (B) A representative visualization of rhamnolipid production of the strains indicated.

is mixed with both RpoN-AlgU (9 genes)-dependent genes and RpoN-only (45 genes)-dependent genes. In terms of organization, the AlgU-RpoN-dependent genes are located near the middle of the operon. Within this core set of genes, *glgA* encodes glycogen synthase. It is possible that AlgU controls storage of carbohydrate supply, whereas RpoN controls catabolism

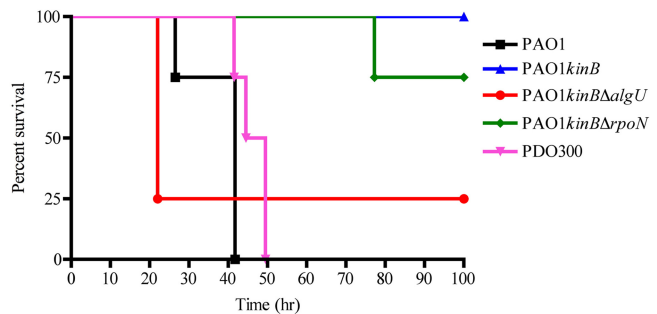


**FIG 5** Survival of BALB/c challenged with *P. aeruginosa* strains. The percent survival of female BALB/c mice is plotted over time ( $n = 8$  mice per group) with each mouse receiving a comparable dose of  $1 \times 10^7$  CFU via intranasal delivery. Statistical analyses were performed using a log rank test, and all strains were compared to PAO1. *P* values for PAO1 compared to the various strains are as follows: *kinB* strain, 0.01; *kinB*  $\Delta$ *algU* strain, 0.6; *kinB*  $\Delta$ *rpoN* strain, 0.01; PDO300 (*mucA22*) strain, 0.1.

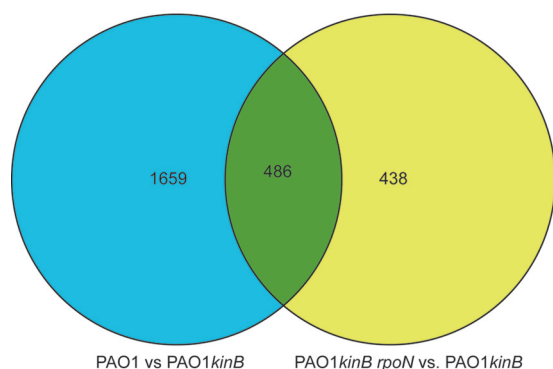


**FIG 6** Venn diagrams comparing the transcriptomes of the strains detailed in this study with additional comparison to wt strain PAO1. The strains in this study (PAO1 *kinB* and PAO1 *kinB*  $\Delta$ *rpoN*) were cultured on PIA; but the PAO1 strain for comparison was cultured in L broth (34).

of glycogen via the PA21XX chromosomal region. It has been demonstrated previously that alginate production by *muc-23* mutant strain PAO579 is nitrogen dependent (5). Interestingly, since most of the PA21XX chromosomal region is RpoN dependent, it seems probable that strains other than the *kinB* strain also utilize this chromosomal region. Our data intercalated with previous studies by other investigators (50, 54, 61) suggest that there may be another tier of regulation above alginate synthesis and MucA proteolysis at the level of management of carbohydrate supply.

Given the number of *P. aeruginosa* two-component systems (47) and sigma factors (44) in the PAO1 genome, it is not hard to imagine many possible gene expression patterns. To the best of our knowledge, this work is the first example of transcriptome and proteome analyses of a strain lacking a sensor kinase and an alternative sigma factor. The unmistakable mucoid phenotype prompted our approach to characterizing the regulation by sensor kinase KinB and sigma factor RpoN. In this study we focused on the regulon controlled by RpoN in the *kinB* mutant. However, there are likely many genes that are differentially regulated due to the loss of *kinB* that are independent of RpoN. In order to determine which genes are directly controlled by KinB, a Venn diagram comparing the transcriptomes of PAO1 versus PAO1 *kinB* to PAO1 *kinB*  $\Delta$ *rpoN* versus PAO1 *kinB* is shown in Fig. 6. There are 486 genes that appear to be directly controlled by KinB despite the fact that the RNA used for the PAO1 *kinB* microarray was isolated from cells cultured on LB agar and that the RNA used for the PAO1 microarray was from cells grown to stationary phase in LB

broth (34). Of note, 80% of genes repressed in PAO1 *kinB*  $\Delta$ *rpoN* compared to PAO1 *kinB* were also repressed in the PAO1 strain compared to PAO1 *kinB*. This diagram also illustrates that there may be far more genes affected by the loss of *kinB* but are independent of *rpoN*.

The *kinB* mutant strain displays a white phenotype dissimilar from *mucA22* strains such as PDO300 (data not shown). Siderophore pyocyanin production does not seem evident on visual inspection of the *kinB* mutant due to the lack of pigment production of the strain on agar medium. Loss of *rpoN* caused a robust up-regulation of pyochelin, which is mostly thought of as the minor siderophore. It seems that the QS system is upregulated to keep the need to acquire iron via pyochelin from the environment. Other investigators have shown that low iron can upregulate QS (31). Furthermore, studies have shown that *rhlAB* (38) and *rhlI* (51) are dependent on RpoN. It has been shown that RpoN negatively regulates QS (27), but, here, in the *kinB* mutant background, iron regulation and QS can be tied together with RpoN.

Recently, a hypothesis has been derived which directly ties nitrogen regulation to quorum sensing (62). In that work, the authors suggest that nitrogen availability alerts the organism to express various factors when metabolically prudent (62). Assimilation of this rule into the data described in this work suggests that loss of *rpoN* may arrest bacteria in a growth phase. Strains PAO1 and PAO1  $\Delta$ *rpoN* do not show visible differences in growth on standard rich culture medium (data not shown), but loss of *rpoN* renders the organism nonmotile. Conversely, deletion of *rpoN* from the *kinB* mutant causes a small-colony variant phenotype (data not shown). These data suggest that *rpoN* may be involved in additional physiological behaviors besides just motility, nitrogen metabolism, and virulence. Our data, as well as those of others, implicate *rpoN* in both direct and indirect mechanisms causing differential gene expression.

The pleiotropic effects of the inactivation of *kinB*, as observed in the transcriptome and proteome, indicate that *kinB* could impact the virulence of the organism. In Table 5 the phenotypic changes of each of the strains are indicated. Previously, we had shown that *algU* and *rpoN* are required for the mucoid phenotype of the *kinB* mutant (12). Our transcriptome analysis indicated that a large region of genes was repressed with the mucoid phenotype (Table 1). This observation was confirmed by both RT-qPCR and iTRAQ proteomic analysis (Tables 3 and 4). Another novel phenotype observed in the *kinB* regulon was the dramatic upregulation of pyochelin biosynthesis genes due to the deletion of *rpoN* (Table 2). Previously, mucoid isolates have been shown to produce less pyo-

**TABLE 5** Summary of *P. aeruginosa* gene classes and phenotypes regulated by KinB and RpoN<sup>a</sup>

Strain	Alginate activity	Carbohydrate <sup>b</sup>	Pyochelin <sup>c</sup>	Relative motility <sup>d</sup>	Rhamnolipids <sup>e</sup>	Virulence <sup>f</sup>
PAO1	Nonmucoid (wt)	wt	wt	Motile (wt)	wt	Virulent (wt)
<i>kinB</i> strain	Mucoid	↑	↓	Nonmotile	↓	Avirulent
<i>kinB</i> $\Delta$ <i>algU</i> strain	Nonmucoid	↓	ND	Motile	ND	Virulent
<i>kinB</i> $\Delta$ <i>rpoN</i> strain	Nonmucoid	↓	↑	Nonmotile	wt	Avirulent

<sup>a</sup> Up and down arrows indicated up- and downregulation, respectively; wt, the level of PAO1.

<sup>b</sup> High numbers of genes which likely play roles in the regulation of carbohydrate metabolism were identified as upregulated in the transcriptome analysis. Expression of these genes was assayed by transcriptome, RT-qPCR, and iTRAQ analyses.

<sup>c</sup> Expression of operons and genes which encode products responsible for synthesizing pyochelin was assayed by transcriptome analysis as well as RT-qPCR. ND, not determined.

<sup>d</sup> Motility was assayed by various methods (Fig. 3A and B).

<sup>e</sup> Rhamnolipid levels were measured (Fig. 4A and B). ND, not determined.

<sup>f</sup> The level of virulence of the respective strain to acute infection leading to mortality of BALB/c mice.



chelin (60). Here, we have observed their upregulation in a nonmucoid *kinB rpoN* mutant (Table 2). Pyochelin production has been shown to increase virulence of a subset of strains (9). These data beg the question as to why pyochelin is differentially regulated in mucoid strains. Since the *kinB* strain is mucoid and has high AlgU activity, we would expect that the *kinB* mutant would be less motile, as other investigators have described (50). We observed low motility for the *kinB rpoN* double mutant as expected and wild-type amounts of swimming and swarming motility for the *kinB algU* mutant (Fig. 3A). However, our analyses did not reveal the RpoN-dependent changes in pilin (*pilA*) (14). It is possible that the expression difference in these mutants was too low to be detected. However, another possibility is that the other phenotypes as noted here, such as rhamnolipid production, may account for this discrepancy. Another interesting change observed in the proteome was the dysregulation of rhamnolipid production (Table 1). Loss of *rpoN* in the mucoid mutant increased rhamnolipid production in the *kinB* mutant (Fig. 4A and B). Due to the variety of phenotypes observed in our study, it seemed pertinent to observe the effect of *kinB* on virulence in an acute pneumonia model (Fig. 5). To our surprise, the *kinB* strain was attenuated in virulence and caused no mortality even though the mucoid strain PDO300 (PAO1 *mucA22*) was just as virulent as PAO1 (Fig. 5). A previous study has shown that inactivation of *algU* causes increased virulence in nonmucoid strain PAO1 (64). This could explain why the *kinB algU* double mutant causes increased mortality compared to the *kinB* mutant. At first glance, Table 5 would seem to indicate that motility and virulence directly correlate. However, both the *kinB* mutant and PDO300 have similar motility levels (data not shown). These data suggest that effect of *kinB* on virulence is not due to the mucoid phenotype or motility but may be attributed to one or more of the other genes of the regulon. Our virulence data with BALB/c mice corroborate the recent observation that *kinB* controls virulence in PA14 against zebrafish embryos (7). In addition to the phenotypes described here, others have shown that KinB regulates pyocyanin, elastase, and biofilm formation (7). Here, we also observed increased expression of elastase (*lasB*) (Tables 2 and 3). Interestingly, the authors of the aforementioned study showed that the kinase activity of KinB was dispensable for virulence (7). Collectively, these data indicate control of the KinB regulon is pleiotropic and complex.

*P. aeruginosa* has a large genome encoding many two-component systems and a vast number of virulence factors (47). *P. aeruginosa* is a danger to the health and well-being of persons living with CF. We have employed “-omic” techniques and phenotypic analyses to describe a regulon of genes controlled by the sensor kinase KinB through direct and indirect pathways. We found that KinB and RpoN control far more genes and phenotypes than we would have imagined. What does this mean in terms of the larger picture of overall pathogenesis of *P. aeruginosa*? At this juncture we could only speculate as to what environmental cues activate KinB to relay signals through AlgB and RpoN to coordinate expression of virulence. The inactivation of KinB resulted in the activation of alginate overproduction (12), and here we observed attenuation of virulence. These data suggest that stable mucoid strains that are not virulent may be useful as attenuated vaccine strains. With its tool box of virulence genes, preventing *P. aeruginosa* infec-

tions may be the best chance for prolonging the lives of CF patients. As proteomic analysis catches up to total transcriptome analysis, the regulation of virulence may become clearer and also increase hope for treatment and control of *P. aeruginosa* opportunistic infection.

## ACKNOWLEDGMENTS

F.H.D. was supported by training grants from the NASA Graduate Student Researchers Program (NNX06AH20H), NASA West Virginia Space Grant Consortium, and a postdoctoral fellowship from the Cystic Fibrosis Foundation (DAMRON10F0). J.P.O. was partially supported by NIH through University of Virginia Infectious Disease training grant AI07406. J.J.V. was supported by the NIH through the University of Virginia Bio-defense Research and Career training grant 5T32AI055432. J.B.G. was supported by grants from the NIH (R01 AI068112) and the Cystic Fibrosis Foundation (GOLDBERG10G0). M.J.S. was supported by NIH R01 AI050812-01. H.D.Y. was supported by the NASA West Virginia Space Grant Consortium, NIH P20 RR016477 to the West Virginia IDeA Network for Biomedical Research Excellence, and the Cystic Fibrosis Foundation (YU11G0). This work was also partially funded by Progenesis Technologies, LLC.

We thank Matt Powell of Protea Biosciences for assistance with the iTRAQ proteomic analysis. We thank Mike Vasil of University of Colorado for the generous gift of the PAO1  $\Delta$ *rhlA* strain and Dennis Ohman of Virginia Commonwealth University for the generous gift strain PDO300. Finally, we also thank the anonymous reviewers for the helpful comments.

## REFERENCES

- Alm RA, Mattick JS. 1995. Identification of a gene, *pilV*, required for type 4 fimbrial biogenesis in *Pseudomonas aeruginosa*, whose product possesses a pre-pilin-like leader sequence. *Mol. Microbiol.* 16:485–496.
- Baynham PJ, Brown AL, Hall LL, Wozniak DJ. 1999. *Pseudomonas aeruginosa* AlgZ, a ribbon-helix-helix DNA-binding protein, is essential for alginate synthesis and *algD* transcriptional activation. *Mol. Microbiol.* 33:1069–1080.
- Baynham PJ, Ramsey DM, Gvozdyev BV, Cordonnier EM, Wozniak DJ. 2006. The *Pseudomonas aeruginosa* ribbon-helix-helix DNA-binding protein AlgZ (AmrZ) controls twitching motility and biogenesis of type IV pili. *J. Bacteriol.* 188:132–140.
- Boucher JC, et al. 1996. Two distinct loci affecting conversion to mucoidy in *Pseudomonas aeruginosa* in cystic fibrosis encode homologs of the serine protease HtrA. *J. Bacteriol.* 178:511–523.
- Boucher JC, Schurr MJ, Deretic V. 2000. Dual regulation of mucoidy in *Pseudomonas aeruginosa* and sigma factor antagonism. *Mol. Microbiol.* 36:341–351.
- Cezairliyan BO, Sauer RT. 2009. Control of *Pseudomonas aeruginosa* AlgW protease cleavage of MucA by peptide signals and MucB. *Mol. Microbiol.* 72:368–379.
- Chand NS, et al. 2011. The sensor kinase KinB regulates virulence in acute *Pseudomonas aeruginosa* infection. *J. Bacteriol.* 193:2989–2999.
- Ciofu O, et al. 2008. Investigation of the *algT* operon sequence in mucoid and non-mucoid *Pseudomonas aeruginosa* isolates from 115 Scandinavian patients with cystic fibrosis and in 88 in vitro non-mucoid revertants. *Microbiology* 154:103–113.
- Cox CD. 1982. Effect of pyochelin on the virulence of *Pseudomonas aeruginosa*. *Infect. Immun.* 36:17–23.
- Damron FH, et al. 2011. Vanadate and triclosan synergistically induce alginate production by *Pseudomonas aeruginosa* strain PAO1. *Mol. Microbiol.* 81:554–570.
- Damron FH, Napper J, Teter MA, Yu HD. 2009. Lipotoxin F of *Pseudomonas aeruginosa* is an AlgU-dependent and alginate-independent outer membrane protein involved in resistance to oxidative stress and adhesion to A549 human lung epithelia. *Microbiology* 155:1028–1038.
- Damron FH, Qiu D, Yu HD. 2009. The *Pseudomonas aeruginosa* sensor kinase KinB negatively controls alginate production through AlgW-dependent MucA proteolysis. *J. Bacteriol.* 191:2285–2295.
- Damron FH, Yu HD. 2011. *Pseudomonas aeruginosa* MucD regulates alginate pathway through activation of MucA degradation via MucP proteolytic activity. *J. Bacteriol.* 193:286–291.



14. Dasgupta N, et al. 2003. A four-tiered transcriptional regulatory circuit controls flagellar biogenesis in *Pseudomonas aeruginosa*. *Mol. Microbiol.* 50:809–824.
15. de Kievit TR, Iglewski BH. 2000. Bacterial quorum sensing in pathogenic relationships. *Infect. Immun.* 68:4839–4849.
16. Deretic V, Dikshit R, Konyecsni WM, Chakrabarty AM, Misra TK. 1989. The *algR* gene, which regulates mucoidy in *Pseudomonas aeruginosa*, belongs to a class of environmentally responsive genes. *J. Bacteriol.* 171:1278–1283.
17. DeVries CA, Ohman DE. 1994. Mucoid-to-nonmucoid conversion in alginate-producing *Pseudomonas aeruginosa* often results from spontaneous mutations in *algT*, encoding a putative alternate sigma factor, and shows evidence for autoregulation. *J. Bacteriol.* 176:6677–6687.
18. Firoved AM, Boucher JC, Deretic V. 2002. Global genomic analysis of AlgU ( $\sigma^E$ )-dependent promoters (sigmulon) in *Pseudomonas aeruginosa* and implications for inflammatory processes in cystic fibrosis. *J. Bacteriol.* 184:1057–1064.
19. Firoved AM, Deretic V. 2003. Microarray analysis of global gene expression in mucoid *Pseudomonas aeruginosa*. *J. Bacteriol.* 185:1071–1081.
20. Firoved AM, Ornatowski W, Deretic V. 2004. Microarray analysis reveals induction of lipoprotein genes in mucoid *Pseudomonas aeruginosa*: implications for inflammation in cystic fibrosis. *Infect. Immun.* 72:5012–5018.
21. Firoved AM, Wood SR, Ornatowski W, Deretic V, Timmins GS. 2004. Microarray analysis and functional characterization of the nitrosative stress response in nonmucoid and mucoid *Pseudomonas aeruginosa*. *J. Bacteriol.* 186:4046–4050.
22. Frisk A, et al. 2004. Transcriptome analysis of *Pseudomonas aeruginosa* after interaction with human airway epithelial cells. *Infect. Immun.* 72:5433–5438.
23. Goldberg JB, Dahnke T. 1992. *Pseudomonas aeruginosa* AlgB, which modulates the expression of alginate, is a member of the NtrC subclass of prokaryotic regulators. *Mol. Microbiol.* 6:59–66.
24. Goldberg JB, Gorman WL, Flynn JL, Ohman DE. 1993. A mutation in *algN* permits *trans* activation of alginate production by *algT* in *Pseudomonas* species. *J. Bacteriol.* 175:1303–1308.
25. Govan JR, Deretic V. 1996. Microbial pathogenesis in cystic fibrosis: mucoid *Pseudomonas aeruginosa* and *Burkholderia cepacia*. *Microbiol. Rev.* 60:539–574.
26. Hershberger CD, Ye RW, Parsek MR, Xie ZD, Chakrabarty AM. 1995. The *algT* (*algU*) gene of *Pseudomonas aeruginosa*, a key regulator involved in alginate biosynthesis, encodes an alternative sigma factor (sigma E). *Proc. Natl. Acad. Sci. U. S. A.* 92:7941–7945.
27. Heurlier K, Denervaud V, Pessi G, Reimann C, Haas D. 2003. Negative control of quorum sensing by RpoN (sigma54) in *Pseudomonas aeruginosa* PAO1. *J. Bacteriol.* 185:2227–2235.
28. Heurlier K, et al. 2004. Positive control of swarming, rhamnolipid synthesis, and lipase production by the posttranscriptional RsmA/RsmZ system in *Pseudomonas aeruginosa* PAO1. *J. Bacteriol.* 186:2936–2945.
29. Ishimoto KS, Lory S. 1989. Formation of pilin in *Pseudomonas aeruginosa* requires the alternative sigma factor (RpoN) of RNA polymerase. *Proc. Natl. Acad. Sci. U. S. A.* 86:1954–1957.
30. Kearns DB, Shimkets LJ. 2001. Directed movement and surface-borne motility of *Myxococcus* and *Pseudomonas*. *Methods Enzymol.* 336:94–102.
31. Kim EJ, Wang W, Deckwer WD, Zeng AP. 2005. Expression of the quorum-sensing regulatory protein LasR is strongly affected by iron and oxygen concentrations in cultures of *Pseudomonas aeruginosa* irrespective of cell density. *Microbiology* 151:1127–1138.
32. Leech AJ, Sprinkle A, Wood L, Wozniak DJ, Ohman DE. 2008. The NtrC family regulator AlgB, which controls alginate biosynthesis in mucoid *Pseudomonas aeruginosa*, binds directly to the *algD* promoter. *J. Bacteriol.* 190:581–589.
33. Lindhout T, Lau PC, Brewer D, Lam JS. 2009. Truncation in the core oligosaccharide of lipopolysaccharide affects flagella-mediated motility in *Pseudomonas aeruginosa* PAO1 via modulation of cell surface attachment. *Microbiology* 155:3449–3460.
34. Lizewski SE, et al. 2004. Identification of AlgR-regulated genes in *Pseudomonas aeruginosa* by use of microarray analysis. *J. Bacteriol.* 186:5672–5684.
35. Ma S, et al. 1998. Phosphorylation-independent activity of the response regulators AlgB and AlgR in promoting alginate biosynthesis in mucoid *Pseudomonas aeruginosa*. *J. Bacteriol.* 180:956–968.
36. Martin DW, et al. 1993. Mechanism of conversion to mucoidy in *Pseudomonas aeruginosa* infecting cystic fibrosis patients. *Proc. Natl. Acad. Sci. U. S. A.* 90:8377–8381.
37. Mathee K, et al. 1999. Mucoid conversion of *Pseudomonas aeruginosa* by hydrogen peroxide: a mechanism for virulence activation in the cystic fibrosis lung. *Microbiology* 145:1349–1357.
38. Medina G, Juarez K, Valderrama B, Soberon-Chavez G. 2003. Mechanism of *Pseudomonas aeruginosa* RhlR transcriptional regulation of the *rhlAB* promoter. *J. Bacteriol.* 185:5976–5983.
39. Miller RM, et al. 2008. *Pseudomonas aeruginosa* twitching motility-mediated chemotaxis towards phospholipids and fatty acids: specificity and metabolic requirements. *J. Bacteriol.* 190:4038–4049.
40. Morici LA, et al. 2007. *Pseudomonas aeruginosa* AlgR represses the Rhl quorum-sensing system in a biofilm-specific manner. *J. Bacteriol.* 189:7752–7764.
41. Morton CO, et al. 2011. The temporal dynamics of differential gene expression in *Aspergillus fumigatus* interacting with human immature dendritic cells in vitro. *PLoS One* 6:e16016.
42. Petrova OE, Schurr JR, Schurr MJ, Sauer K. 2011. The novel *Pseudomonas aeruginosa* two-component regulator BfmR controls bacteriophage-mediated lysis and DNA release during biofilm development through PhdA. *Mol. Microbiol.* 81:767–783.
43. Pinzon NM, Ju LK. 2009. Analysis of rhamnolipid biosurfactants by methylene blue complexation. *Appl. Microbiol. Biotechnol.* 82:975–981.
44. Potvin E, Sanschagrin F, Levesque RC. 2008. Sigma factors in *Pseudomonas aeruginosa*. *FEMS Microbiol. Rev.* 32:38–55.
45. Qiu D, Eisinger VM, Rowen DW, Yu HD. 2007. Regulated proteolysis controls mucoid conversion in *Pseudomonas aeruginosa*. *Proc. Natl. Acad. Sci. U. S. A.* 104:8107–8112.
46. Ramsey DM, Wozniak DJ. 2005. Understanding the control of *Pseudomonas aeruginosa* alginate synthesis and the prospects for management of chronic infections in cystic fibrosis. *Mol. Microbiol.* 56:309–322.
47. Rodrigue A, Quentin Y, Lazdunski A, Mejean V, Foglino M. 2000. Two-component systems in *Pseudomonas aeruginosa*: why so many? *Trends Microbiol.* 8:498–504.
48. Rowen DW, Deretic V. 2000. Membrane-to-cytosol redistribution of ECF sigma factor AlgU and conversion to mucoidy in *Pseudomonas aeruginosa* isolates from cystic fibrosis patients. *Mol. Microbiol.* 36:314–327.
49. Schuster M, Lostroh CP, Ogi T, Greenberg EP. 2003. Identification, timing, and signal specificity of *Pseudomonas aeruginosa* quorum-controlled genes: a transcriptome analysis. *J. Bacteriol.* 185:2066–2079.
50. Tart AH, Wolfgang MC, Wozniak DJ. 2005. The alternative sigma factor AlgT represses *Pseudomonas aeruginosa* flagellum biosynthesis by inhibiting expression of *fleQ*. *J. Bacteriol.* 187:7955–7962.
51. Thompson LS, Webb JS, Rice SA, Kjelleberg S. 2003. The alternative sigma factor RpoN regulates the quorum sensing gene *rhlI* in *Pseudomonas aeruginosa*. *FEMS Microbiol. Lett.* 220:187–195.
52. Totten PA, Lara JC, Lory S. 1990. The *rpoN* gene product of *Pseudomonas aeruginosa* is required for expression of diverse genes, including the flagellin gene. *J. Bacteriol.* 172:389–396.
53. Waite RD, et al. 2006. Clustering of *Pseudomonas aeruginosa* transcriptomes from planktonic cultures, developing and mature biofilms reveals distinct expression profiles. *BMC Genomics* 7:162.
54. Waite RD, Papakonstantinou A, Littler E, Curtis MA. 2005. Transcriptome analysis of *Pseudomonas aeruginosa* growth: comparison of gene expression in planktonic cultures and developing and mature biofilms. *J. Bacteriol.* 187:6571–6576.
55. Waters CM, Bassler BL. 2005. Quorum sensing: cell-to-cell communication in bacteria. *Annu. Rev. Cell Dev. Biol.* 21:319–346.
56. Winsor GL, et al. 2009. *Pseudomonas* genome database: facilitating user-friendly, comprehensive comparisons of microbial genomes. *Nucleic Acids Res.* 37:D483–D488.
57. Wood LF, Leech AJ, Ohman DE. 2006. Cell wall-inhibitory antibiotics activate the alginate biosynthesis operon in *Pseudomonas aeruginosa*: roles of sigma (AlgT) and the AlgW and Prc proteases. *Mol. Microbiol.* 62:412–426.
58. Wood LF, Ohman DE. 2006. Independent regulation of MucD, an HtrA-like protease in *Pseudomonas aeruginosa*, and the role of its proteolytic motif in alginate gene regulation. *J. Bacteriol.* 188:3134–3137.
59. Wood LF, Ohman DE. 2009. Use of cell wall stress to characterize sigma

- 22 (AlgT/U) activation by regulated proteolysis and its regulon in *Pseudomonas aeruginosa*. *Mol. Microbiol.* 72:183–201.
60. Woods DE, et al. 1991. In vivo regulation of virulence in *Pseudomonas aeruginosa* associated with genetic rearrangement. *J. Infect. Dis.* 163:143–149.
61. Wu W, Badrane H, Arora S, Baker HV, Jin S. 2004. MucA-mediated coordination of type III secretion and alginate synthesis in *Pseudomonas aeruginosa*. *J. Bacteriol.* 186:7575–7585.
62. Xavier JB, Kim W, Foster KR. 2011. A molecular mechanism that stabilizes cooperative secretions in *Pseudomonas aeruginosa*. *Mol. Microbiol.* 79:166–179.
63. Yorgey P, Rahme LG, Tan MW, Ausubel FM. 2001. The roles of *mucD* and alginate in the virulence of *Pseudomonas aeruginosa* in plants, nematodes and mice. *Mol. Microbiol.* 41:1063–1076.
64. Yu H, Boucher JC, Hibler NS, Deretic V. 1996. Virulence properties of *Pseudomonas aeruginosa* lacking the extreme-stress sigma factor AlgU ( $\sigma^E$ ). *Infect. Immun.* 64:2774–2781.